Molecular Biology of the Cell
Vol. 13, 1566–1581, May 2002

Probing for Membrane Domains in the Endoplasmic Reticulum: Retention and Degradation of Unassembled MHC Class I Molecules

Elias T. Spiliotis, Tsvetelina Pentcheva, and Michael Edidin*

Department of Biology, The Johns Hopkins University, Baltimore, Maryland 21218

Submitted June 28, 2001; Revised January 23, 2002; Accepted February 1, 2002
Monitoring Editor: Chris Kaiser

Quality control of protein biosynthesis requires ER-retention and ER-associated degradation (ERAD) of unassembled/misfolded molecules. Although some evidence exists for the organization of the ER into functionally distinct membrane domains, it is unknown if such domains are involved in the retention and ERAD of unassembled proteins. Here, it is shown that unassembled MHC class I molecules are retained in the ER without accumulating at ER-exit sites or in the ERGIC of $\beta 2m^{-/-}$ cells. Furthermore, these molecules did not cluster in the ER membrane and appeared to be highly mobile even when ERAD or their association with calnexin were inhibited. However, upon ATP depletion, they were reversibly segregated into an ER membrane domain, distinct from ER exit sites, which included calnexin and COPII, but not the ERGIC marker protein p58. This quality control domain was also observed upon prolonged inhibition of proteasomes. Microtubules were required for its appearance. Segregation of unfolded proteins, ER-resident chaperones, and COPII may be a temporal adaptation to cell stress.

INTRODUCTION

Major histocompatibility complex (MHC) class I molecules consist of a transmembrane heavy chain, a soluble β2-microglobulin (β2m) light chain, and an 8–10 residue peptide. Assembly of MHC class I heterotrimers occurs in the endoplasmic reticulum (ER) and involves binding to the ER-resident chaperones calnexin, calreticulin and ERp57, and a peptide-loading complex comprising the transporter associated with antigen processing and tapasin (Cresswell *et al.*, 1999). Assembly begins with noncovalent association of MHC class I heavy chains with β2m; this is facilitated by their interaction with calnexin and calreticulin. In the absence of β2m, unassembled/misfolded MHC class I molecules are retained in the ER, and they are extruded into the cytosol where they are deglycosylated and degraded by the proteasome (Sege *et al.*, 1981; Hughes *et al.*, 1997).

ER retention of misfolded proteins occurs either by their retrieval from post-ER compartments (ERGIC and/or *cis*-Golgi) or by their exclusion from sites of vesicle formation for ER exit (Ellgaard *et al.*, 1999). The intramembrane mechanism of ER retention can be either dynamic or static. Misfolded vesicular stomatitis virus G (VSVG) proteins have been observed to diffuse freely in the ER membrane, and this may reflect their dynamic association with and dissociation from calnexin and BiP (Cannon and Helenius, 1999; Nehls *et al.*, 2000). In contrast, other unassembled proteins may interact with ER resident chaperones that are part of a relatively immobile ER matrix (Tatu and Helenius, 1997; Lee *et al.*, 1999; Marguet *et al.*, 1999). A static mechanism can also involve the aggregation of misfolded proteins into complexes that are too large to be packaged into ER-budding vesicles (Rivera *et al.*, 2000).

Prolonged retention of unassembled or misfolded proteins in the ER is followed by their degradation. ER-associated degradation (ERAD) entails recognition of terminally misfolded proteins by ER-resident chaperones, retrotranslocation into the cytosol, and degradation by the proteasome after deglycosylation and ubiquitination (Ellgaard *et al.*, 1999). Differential mannose trimming by ER mannosidases I and II has been proposed to signal the degradation of terminally misfolded glyproteins (Liu *et al.*, 1999; Cabral *et al.*, 2000). Recent studies have shown that ERAD is suppressed upon inhibiting the activity of ER mannosidases (Liu *et al.*, 1999; Tokunaga *et al.*, 2000; Wang and White, 2000). Retrotranslocation of misfolded proteins into the cytosol appears to occur concurrently with their degradation by the proteasome. Several studies have shown that upon inhibition of proteasomal activity, misfolded proteins do not translocate into the cytosol, and they remain intact in the secretory pathway (Hirsch and Ploegh, 2000).

Although ER retention and ERAD of misfolded proteins are processes that occur in tandem, they are mostly studied as separate phenomena, and it is unknown how ERAD may sustain or contribute to mechanisms of ER retention. Fur-

DOI: 10.1091/mbc.01–07–0322.
* Corresponding author. E-mail address: edidin@jhu.edu.

thermore, it is unknown how the ER membrane is organized to facilitate ER retention and ERAD of misfolded proteins. Some biochemical and ultrastructural evidence exists for the organization of the ER into restricted and perhaps functionally distinct membrane domains (Pryme, 1986; Vertel *et al.*, 1992; Baumann and Walz, 2001), but no studies have probed for the accumulation of misfolded proteins at such membrane domains.

Here, we investigate the intramembrane mechanism by which unassembled mouse MHC class I, $H2K^b$ molecules are retained in the ER of fibroblast cells from β2m knock-out mice (Koller *et al.* 1990; Zijlstra *et al.*, 1990). To probe for membrane domains, unassembled $H2K^b$ molecules were imaged at a resolution of <100 Å by fluorescence resonance energy transfer (FRET), and their diffusion was measured by fluorescence recovery after photobleaching (FRAP). Unassembled MHC class I molecules diffused freely and were randomly distributed in the ER membrane of $\beta2m^{-/-}$ cells even when calnexin-association and ERAD were inhibited. However, when cells were depleted of ATP, MHC class I molecules accumulated at an ER subdomain that included calnexin and COPII.

MATERIALS AND METHODS

Cells and DNA Constructs

Primary fibroblast cells from $\beta2m^{-/-}$ mice were passaged twice, and they were transfected with a plasmid (*pRSV-TAg*) encoding for the SV40 (SV40) T-Ag, a kind gift of Dr. Stephen Gould (Johns Hopkins School of Medicine). Cells were passaged once, and they were fed every 2–4 d with DMEM supplemented with glucose and 20% fetal bovine serum (FBS). After the formation of foci, cells were trypsinized. The mixture was placed in a conical tube, and it was left undisturbed until the foci had settled to the bottom of the tube. The top 80% of the supernatant was discarded. The foci along with the remaining 20% of the supernatant were plated and fed for another 2 weeks to select for transformed cells. At the end of this period, cells from the newly harvested foci were expanded in a continuous culture. Frozen stocks were made, and the new cell line was designated as $\beta2m^{-/-}$ cells. Stable cell lines ($\beta2m^{-/-}K^bGFP$) were produced by transfecting $\beta2m^{-/-}$ cells with *pH2K^{b}GFP* (Spiliotis *et al.*, 2000). Cells were transfected using LipofectAMINE reagent (Life Technologies, Rockville, MD), then selected for G418 resistance, and cloned. These cells lines were maintained by 1:10 passage three to four times weekly in DMEM supplemented with glucose, 15% FBS.

Transient transfections of $\beta2m^{-/-}$ cells were established using 2 μg of *pH2L^{d}untag* (Marguet *et al.*, 1999) per 6 μl of the FuGENE reagent (Roche Molecular Biochemicals, Indianapolis, IN). L-cells were maintained as previously described (Marguet *et al.*, 1999), and they were transiently transfected using 2 μg of *pH2K^{b}GFP* per 6 μl of the FuGENE reagent. For FRET experiments, $\beta2m^{-/-}$ cells were plated onto coverslips for 24 h, and subsequently they were transfected with *pH2K^{b}YFP* and *pH2K^{b}CFP* at ratios of 1:1 (1 μg:1 μg), 2:1 (1 μg:0.5 μg), and 1:2 (1 μg:0.5 μg) per each 6 μl of the FuGENE reagent.

The *pH2K^{b}YFP* and *pH2K^{b}CFP* constructs were made by excising the EGFP from *pH2K^{b}GFP* using the restriction enzymes *Bam*HI and *Bsr*GI (New England Biolabs). The remaining linear DNA of *pH2K^{b}GFP* was ligated to the *Bam*HI/*Bsr*GI fragments of *pYFP-N3* and *pCFP-N3* (Pentcheva and Edidin, 2001).

Where indicated, cells were incubated in medium supplemented with 1 mM castanospermine (Sigma Chemical, St. Louis, MO), 1 mM swainsonine (Calbiochem, La Jolla, CA), 1 mM kifunensine (Calbiochem), 20 μM lactacystin (Kamiya Biomedical, Thousand Oaks, CA). In ATP-depletion experiments, cells were incubated in glucose- and sodium pyruvate-free DMEM (Life Technologies) supplemented with 50 mM 2-deoxy-D-glucose (Sigma) and 0.02% sodium azide (Sigma). Where indicated, cell media were supplemented with 33 μM nocodazole (Sigma).

Table 1. Diffusion coefficients (D) and mobile fraction (R) for $H2K^bGFP$ in $\beta2m^{-/-}$ cells

Treatment	D ($\times10^{-10}$ cm^2 s^{-1})	R (%)
—	40 ± 3	83 ± 5
cas	42 ± 3	90 ± 4
swn/kif	41 ± 3	87 ± 7
lac	44 ± 2	83 ± 3
dog	40 ± 4	39 ± 12

Values are ± 95% confidence limits. cas, 1 mM castanospermine; swn/kif, 1 mM swainsonine, 1 mM kifunensine; lac, 20 μM lactacystin; dog, 50 mM 2-deoxy-D-glucose and 0.02% sodium azide in glucose-free medium.

Confocal Microscopy

Cells were fixed for 30 min at room temperature with 4% paraformaldehyde in PBS. After washing with 0.25% NH_4Cl in PBS, cells were permeabilized in PBS containing 0.2% saponin and 1% BSA. This solution was also used for all antibody dilutions and washes. Rabbit anti-p137 (Shugrue *et al.*, 1999) was the gift of Dr. Ann Hubbard (Johns Hopkins School of Medicine); it was diluted at 1:1000. Rabbit anti-p58 (Saraste and Svensson, 1991) was donated by Dr. Jaakko Saraste (University of Bergen, Norway); it was used at 1:50. Rabbit anti–α-mannosidase II (Velasco *et al.*, 1993) was the gift of Dr. Marilyn Farquhar (University of California, San Diego); it was diluted at 1:800. A rabbit anticalnexin carboxy terminus polyclonal antibody (StressGen, Victoria, British Columbia, Canada) was diluted at 1:200. mAb 64-3-7 (Shiroishi *et al.*, 1985) was the kind gift of Dr. Ted Hansen (Washington University School of Medicine), and it was used at 20 μg/ml. Rabbit anti-UDPGlc:glycoprotein glucosyltransferase (Zuber *et al.*, 2001) was kindly donated by Dr. Armando Parodi (University of San Martin, Buenos Aires, Argentina); it was diluted at 1:200. The Cy5-conjugated $F(ab')_2$ donkey anti-rabbit and anti-mouse IgG (H+L), and the Alexa 488—conjugated $F(ab')_2$ goat anti-rabbit (H+L) reagents (Jackson ImmunoResearch Laboratories, West Grove, PA) were used at 10 μg/ml. An ethanol stock (1 mg/ml) of DiOC6 (Molecular Probes, Eugene, OR) was diluted at 200 ng/ml, and it was immediately added to permeabilized cells for no longer than 30 s. Before staining, antibodies were airfuged at 80,000 rpm. Coverslips were mounted onto glass slides in antifade solution containing 0.1% DABCO (Sigma) and 90% glycerol. Samples were imaged on a confocal laser scanning microscope (Leica TCS SP, Deerfield, IL) from ~1-μm optical sections.

Measurements of Lateral Diffusion by FRAP

Before each experiment, $\beta2m^{-/-}K^bGFP$ cells were grown on coverslips for 2 days. 'Untreated and drug-treated cells (see Table 1) were washed twice in Hanks balanced salt solution (Life Technologies), supplemented with 1% FBS and 10 mM HEPES (pH 7.3). Cells were mounted on slides in the same solution containing castanospermine, swainsonine, kifunensine, or lactacystin, and they were sealed with nail polish. Measurements of lateral diffusion were performed at 37°C for no longer than 45 min per each newly mounted coverslip. After incubation of cells in ATP-depletion medium for 30 min, measurements of lateral diffusion were performed in glucose-free medium containing 50 mM 2-deoxy-D-glucose and 0.02% sodium azide for no longer than 30 min.

Measurements of lateral diffusion, data collection, and analysis were all as previously described (Marguet *et al.*, 1999). D and R were derived from more than 25 measurements per each condition.

FRET Microscopy

Cells were fixed with 4% paraformaldehyde in PBS for 30 min at room temperature. After washing with PBS, cells were incubated for 10 min in equilibration buffer from the SlowFade Light antifade kit (Molecular Probes). Coverslips were mounted on slides in antifade from the same kit and sealed with nail polish.

Cells were imaged on a Zeiss Axiovert 135 TV microscope (Carl Zeiss, Inc., Thornwood, NY) using a 1.4 NA ×100 Zeiss Planapochromat objective. Fluorescence was exited with a 75-W arc lamp. CFP and YFP were detected with XF114 and XF30 filter sets, respectively (Omega Optical, Brattleboro, VT). Digital images were collected with a 12-bit Series 300 cooled CCD (Roper Scientific, Tucson, AZ), operated by the IC300 digital imaging system (Inovision, Raleigh, NC). During the course of a FRET experiment, four images were acquired in the following sequence: 1) an image of the CFP fluorescence; 2) an image of the YFP fluorescence; 3) another image of the YFP fluorescence after 30 s of continuous excitation (photobleaching); and 4) an image of the CFP fluorescence after the photobleaching of YFP. Data were collected from more than 10 fields per coverslip.

Image registration and data analysis were all exactly as previously described (Pentcheva and Edidin, 2001).

Immunoprecipitations, Western Blots, and Pulse-chase

Cells were lysed in buffer containing 1% CHAPS (Sigma), 0.15 M NaCl, 0.05 M Tris-HCl (pH 7.5), 1 mM PMSF, and protease inhibitors. Postnuclear supernatants were precleared with protein A-Sepharose beads (Sigma) and incubated with rabbit anticalnexin (StressGen), and then protein complexes were recovered by incubating with protein A-Sepharose beads. Beads were washed five times in buffer containing 0.1% CHAPS and eluted in 0.2% SDS and 0.125 M Tris-HCl (pH 6.8).

Immunoprecipitates and whole lysates were run on SDS-PAGE and transferred to OPTITRAN membranes (Schleicher & Schuell, Keene, NH). Membranes were incubated with anticalnexin (StressGen), anti-GFP (Molecular Probes), anti-Grp78 (BiP; StressGen) or antiactin (Research Diagnostics, Flanders, NJ) in PBS containing 0.05% Tween-20 and 5% nonfat dry milk. Subsequently, they were washed in PBS/0.05% Tween-20 and incubated with horseradish peroxidase–conjugated anti-rabbit or anti-mouse Ig (Amersham Corp., Arlington Heights, IL). After washing in PBS/0.3% Tween-20, membranes were incubated with ECL detection reagents (Amersham Corp.) and applied to BioMax MR films (Eastman-Kodak, Rochester, NY).

For pulse-chase experiments, 3 million cells were starved for 45 min in methionine- and cysteine-free DMEM (Life Technologies) containing 5% dialyzed FBS, pulsed with ~500 μCi/ml Tran^{35}S-label for 20 min, and chased for 4 h in medium containing 3 mM L-methionine and 3 mM cysteine. Where indicated, all cell media were supplemented with 25 μM lactacystin. Cells were lysed in buffer containing 0.5% Triton X-100 (Sigma), and postnuclear supernatants were precleared with protein G-agarose beads (Sigma). To recover unassembled H2K^b molecules, excess of β2m and 10 μg/ml high-affinity affinity peptide SIY were added to each lysate. Lysates were incubated with mAb 20-8-4 (binds to the α1 domain of β2m-associated H2K^b heavy chains; Williams *et al.*, 1989) and the immune complexes were recovered with protein G-agarose, washed in buffer containing 0.1% Triton X-100, and eluted at 95°C. After residual mAb 20-8-4 was removed by incubating twice with protein G-agarose, lysates were treated with anticalnexin antiserum (StressGen). Eluates were analyzed by 10% SDS-PAGE and autoradiography. The autoradiographs were scanned using Adobe Photoshop (Adobe Systems, San Jose, CA), and densitometric analysis was performed using NIH Image software.

RESULTS

ER-retention of Unassembled MHC Class I Molecules by Exclusion from ER-exit Sites and the ERGIC

The mechanism by which unassembled MHC class I heavy chains are retained in the ER because of lack of association with β2m has been studied only in interferon-γ–inducible carcinoma cell lines (Hsu *et al.*, 1991). These cell lines have been useful in identifying aspects of MHC class I assembly and retention in the ER; however, they are characterized by defective expression of intracellular factors, whose function maybe essential in protein synthesis and export from the ER (Klar and Hammerling, 1989). To study ER retention of MHC class I heavy chains in the specific absence of β2m, primary fibroblast cells from β2m knock-out mice (Koller *et al.*, 1990; Zijlstra *et al.*, 1990) were transformed with the SV40 T-antigen. The new cell line was stably transfected with H2K^{b}GFP, a functional H2K^b chimera with the GFP attached to the C′-terminal end of its cytoplasmic tail (Spiliotis *et al.*, 2000).

To see if unassembled MHC class I proteins are retained in the ER by recycling from the ERGIC or by exclusion from ER-exit sites, the intracellular distribution of H2K^{b}GFP molecules was imaged by confocal microscopy. Green fluorescent H2K^b molecules were uniformly distributed throughout the cytosol in a reticular pattern including a brightly stained nuclear envelope (Figure 1, A and G). H2K^{b}GFP molecules were not localized to post-ER compartments, as shown by staining for p137, a component of the COPII coat that localizes to ER exit sites (Shugrue *et al.*, 1999), and for p58, the rodent homologue of ERGIC53 (Saraste and Svensson, 1991; Figure 1, C and I). To see if this was due to rapid recycling of MHC class I molecules between the ERGIC and the ER, cells were incubated at 15°C to block ER-to-Golgi transport at the level of ERGIC (Saraste and Svensson, 1991; Plutner *et al.*, 1992). In addition, protein synthesis was inhibited to chase H2K^{b}GFP molecules out of the ER and into the ER-exit sites or the ERGIC. Consistent with previous observations (Hammond and Glick, 2000), this treatment resulted in the proliferation of p137-containing elements, which appeared in juxtanuclear structures that resemble the ERGIC (Figure 1E). Although H2K^{b}GFP fluorescence was somewhat more concentrated in the area of the ERGIC than in the rest of the cell (Figure 1F; bold arrowhead), MHC class I molecules maintained a reticular distribution and were excluded from many p137-containing puncta (Figure 1F, thin arrow). On prolonged incubation of cells at 15°C without inhibiting protein synthesis, H2K^{b}GFP molecules remained mainly in the ER, and several p58-containing elements of the ERGIC were free of any H2K^{b}GFP fluorescence (Figure 1L).

To control for artifacts from the use of GFP-tagged probes and to rule out the possibility that these findings were specific to MHC molecules of the H2K^b allele, a similar set of experiments was performed on cells that transiently expressed unmodified H2L^d heavy chains. Intracellular distribution of H2L^d molecules (Figure 2, B and H) was revealed by staining of cells with the conformation-specific mAb 64-

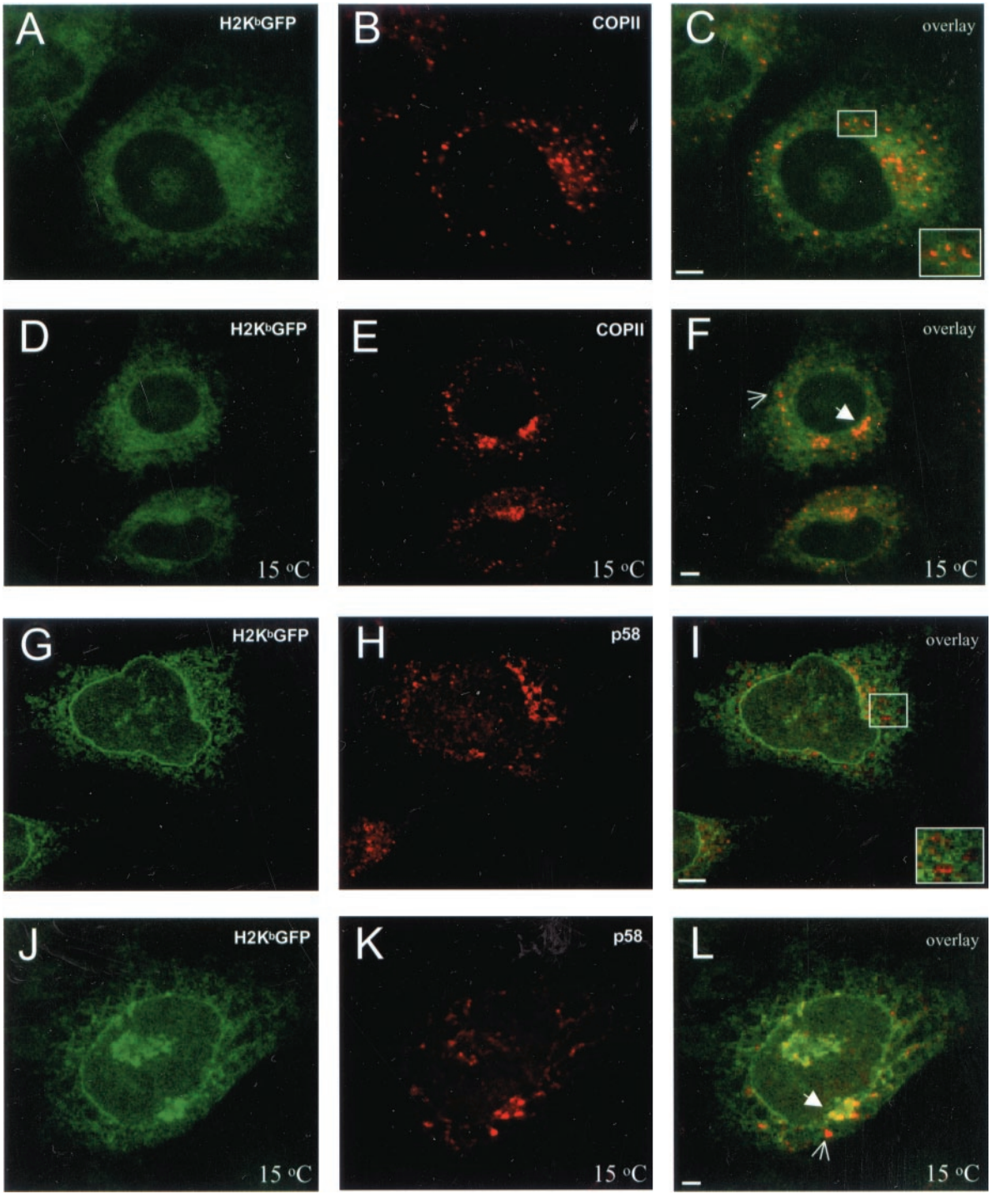

Figure 1. Localization of unassembled H2K^{b}GFP molecules with respect to ER-exit sites and the ERGIC. $\beta2m^{-/-}$K^{b}GFP cells were fixed, permeabilized, and stained with anti-p137 and Cy5-conjugated anti-rabbit Ig. (A) H2K^{b}GFP; (B) p137; and (C) overlay of A and B. $\beta2m^{-/-}$K^{b}GFP cells were treated with cycloheximide (150 μg/ml) at 15°C for 90 min, fixed, permeabilized, and stained with anti-p137 and Cy5-conjugated anti-rabbit Ig. (D) H2K^{b}GFP; (E) p137; and (F) overlay of D and E. $\beta2m^{-/-}$K^{b}GFP cells were fixed, permeabilized, and stained with anti-p58 and Cy5-conjugated anti-rabbit Ig. (G) H2K^{b}GFP; (H) p58; and (I) overlay of G and H. $\beta2m^{-/-}$K^{b}GFP cells were incubated at 15°C for 180 min, fixed, permeabilized, and stained with anti-p58 and Cy5-conjugated anti-rabbit Ig. (J) H2K^{b}GFP; (K) p58; and (L) overlay of J and K. Insets, higher magnification of perinuclear regions containing several ER-exit sites and ERGIC elements; thin arrows, p137- and p58-containing elements that were free of H2K^{b}GFP; bold arrowheads, ER-exit sites and ERGIC elements that included H2K^{b}GFP. All images represent ~1-μm optical sections obtained by confocal microscopy. Scale bars, ~5 μm.

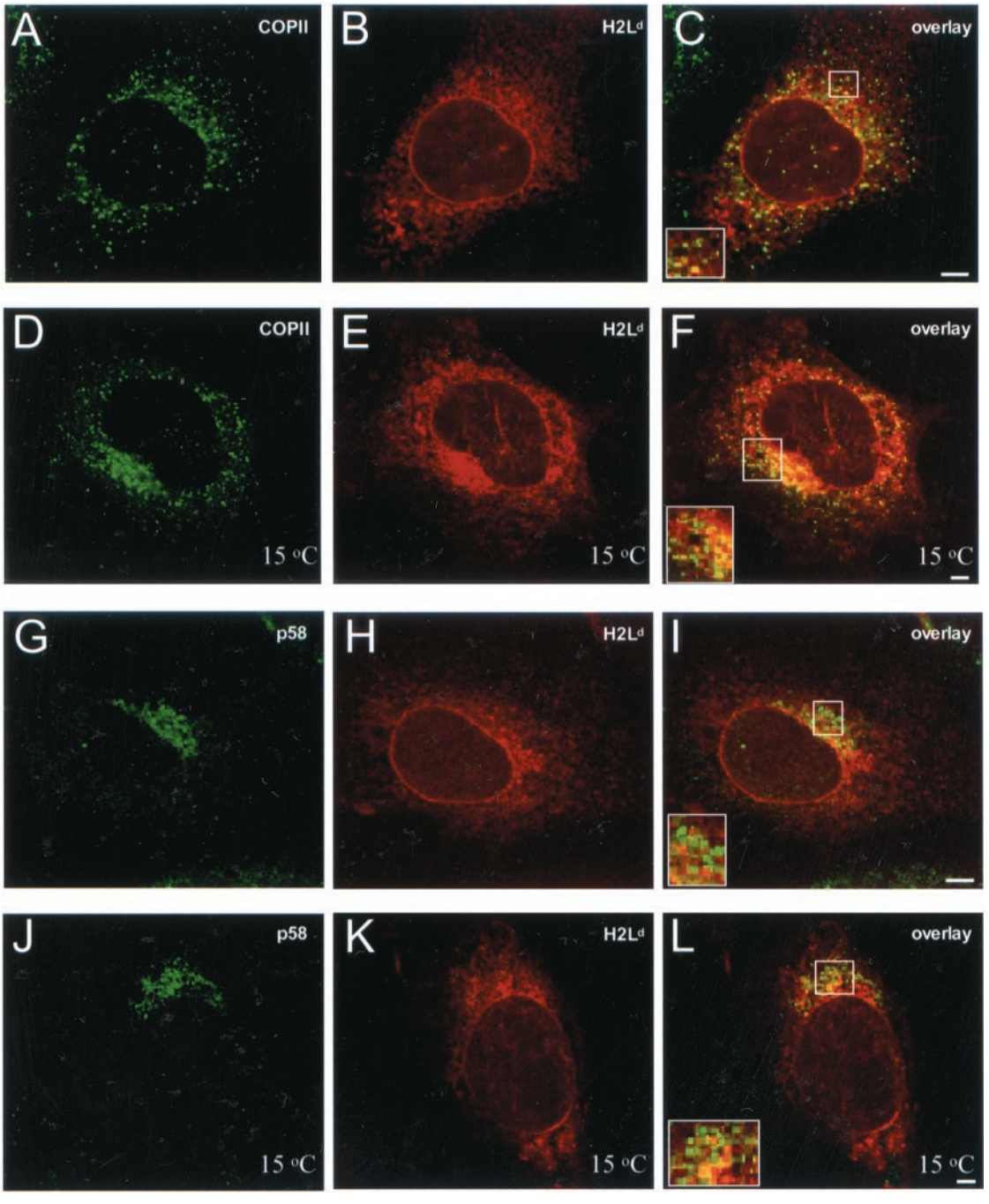

Figure 2. Localization of unassembled native H2L^d molecules with respect to ER-exit sites and the ERGIC. $\beta 2m^{-/-}$ cells were transfected with *H2L^d*; 36 h later, they were fixed, permeabilized, and stained with anti-p137 and mAb 64-3-7 (antiunfolded H2L^d). Samples were sequentially stained with Alexa 488–conjugated anti-rabbit Ig and Cy5-conjugated anti-mouse Ig. (A) p137; (B) H2L^d; and (C) overlay of A and B. $\beta 2m^{-/-}$ cells were transfected with *H2L^d*; 36 h later, they were incubated at 15°C for 180 min, fixed, permeabilized, and stained with anti-p137 and mAb 64-3-7 (antiunfolded H2L^d). Samples were sequentially stained with Alexa 488–conjugated anti-rabbit Ig and Cy5-conjugated anti-mouse Ig. (D) p137; (E) H2L^d; and (F) overlay of D and E. $\beta 2m^{-/-}$ cells were transfected with *H2L^d*; 36 h later, they were fixed, permeabilized, and stained with anti-p58 and mAb 64-3-7 (antiunfolded H2L^d). Samples were sequentially stained with Alexa 488–conjugated anti-rabbit Ig and Cy5-conjugated anti-mouse Ig. (G) p58; (H) H2L^d; and (I) overlay of G and H. $\beta 2m^{-/-}$ cells were transfected with *H2L^d*; 36 h later, they were incubated at 15°C for 180 min, fixed, permeabilized, and stained with anti-p58 and mAb 64-3-7 (antiunfolded H2L^d). Samples were sequentially stained with Alexa 488–conjugated anti-rabbit Ig and Cy5-conjugated anti-mouse Ig. (J) p58; (K) H2L^d; and (L) overlay of J and K. Insets, higher magnification of perinuclear regions containing several ER-exit sites and ERGIC elements. All images represent ~1-μm optical sections obtained by confocal microscopy. Scale bars, ~5 μm.

3-7 (Lie *et al.*, 1991); it was identical to the reticular pattern of $H2K^bGFP$. Although some $H2L^d$ molecules were localized to ER-exit sites (Figure 2C; yellow puncta) and to the ERGIC (Figure 18I; yellow puncta), most of these elements were free of $H2L^d$ (see separate green and red elements in the insets of Figure 2, C and I). The 15°C temperature block of ER-to-Golgi traffic had an effect similar to that observed for $H2K^bGFP$. There was some concentration of $H2L^d$ molecules at p137- (Figure 2E) and p58-containing structures (Figure 2K), but most remained distributed in the reticular pattern characteristic of ER localization. In addition, many sites of the transitional ER and the ERGIC appeared to be free of $H2L^d$ molecules (see green elements in the insets of Figure 2, F and L). These data suggest that the dominant mechanism by which unassembled MHC class I molecules are retained in the ER does not involve rapid recycling between the ERGIC and the ER or significant accumulation at a specialized subcompartment of the ER.

Free Diffusion and Random Distribution of Unassembled MHC Class I Molecules in the ER Membrane of β2m$^{-/-}$ Cells

To see if exclusion from ER-exit sites was due to immobilization, aggregation, or clustering at distinct membrane domains, the intramembrane mobility and distribution of unassembled/misfolded molecules were quantitatively imaged by FRAP and FRET, respectively.

In measurements of lateral mobility by FRAP, a diffusion coefficient, D, is derived from the half-time of fluorescence recovery, and it shows how fast molecules diffuse within the membrane bilayer. The extent of fluorescence recovery (mobile fraction, R) indicates the percentage of molecules that are free to diffuse and/or the existence of disconnected membrane domains. If unassembled/misfolded MHC class I molecules associate with immobile or slowly diffusing proteins, their apparent D should be lower than the one reported for their fully assembled counterparts (Marguet *et al.*, 1999). If they aggregate or associate with immobile proteins irreversibly, their mobile fraction, R, should be low (Nehls *et al.*, 2000). Alternatively, segregation of molecules into membrane subregions should also result in low mobile fractions (Yechiel and Edidin, 1987).

The diffusion of $H2K^bGFP$ in the ER of $\beta2m^{-/-}$ cells, $D = 40 \pm 3 \times 10^{-10}$ cm^2 s^{-1} and $R = 83 \pm 5\%$ (see Table 1 for a summary of all D and R), was similar to the diffusion of $H2K^bGFP$ and $H2L^dGFP$ molecules, after assembly and dissociation from TAP in wild-type L-cells (Marguet *et al.*, 1999; Spiliotis *et al.*, 2000). The intramembrane mobility of unassembled $H2K^bGFP$ molecules was also reminiscent of the high mobile fraction and rapid diffusion of misfolded VSVG-GFP molecules in the ER of COS-7 (Nehls *et al.*, 2000). These measurements suggested that a dynamic interaction with ER-resident chaperones or with components of the ERAD machinery may mediate ER-retention of unassembled/misfolded MHC class I molecules. To identify which one of these components may be responsible for the dynamic mode of ER retention, a pharmacological approach was taken to inhibit association of MHC class I molecules with calnexin and to suppress ERAD.

$\beta2m^{-/-}$ cells were treated with castanospermine (cas), an inhibitor of oligosaccharide processing that has been shown to disrupt class I-calnexin interaction and to impair folding of class I heavy chains (Vassilakos *et al.*, 1996). Indeed, coimmunoprecipitation of calnexin-class I complexes followed by Western blotting with antisera for calnexin and GFP showed a threefold decrease in the number of $H2K^bGFP$ molecules associated with calnexin (Figure 3A). Surprisingly, this effect was not accompanied by a reduction in the intramembrane mobility of unassembled/misfolded molecules, which maintained rapid diffusion and a high percentage of mobile molecules ($D = 42 \pm 3 \times 10^{-10}$ cm^2 s^{-1} and $R = 90 \pm 4\%$).

Because expression of the ER-lumenal chaperone BiP has been reported to increase upon treatment of cells with castanospermine (Balow *et al.*, 1995; Pahl and Baeuerle, 1995), detergent extracts of $\beta2m^{-/-}$ cells were blotted for BiP and actin, which served as an internal control for equivalency of protein content (Figure 3B). The relative amount of BiP protein was found to be 30% higher in castanospermine-treated than in untreated $\beta2m^{-/-}$ cells (Figure 3B). However, an interaction between MHC class I molecules and BiP was unlikely to compensate for diminished association with calnexin. Consistent with other reports (Nossner and Parham, 1995), murine MHC class I heavy chains did not appear to associate with BiP.

To suppress ERAD of unassembled MHC class I molecules, $\beta2m^{-/-}$ cells were treated with kifunensine and swainsonine, which inhibit the enzymatic activities of ER mannosidase I and II, respectively (Gonzalez *et al.*, 1999; Cabral *et al.*, 2000). Although a slight (~10%) decrease was observed in their association with calnexin (Figure 3A), diffusion and mobile fraction of $H2K^bGFP$ molecules were not significantly affected (Table 1). Furthermore, high mobility of $H2K^bGFP$ proteins persisted upon treatment of $\beta2m^{-/-}$ cells with lactacystin, which is known to inhibit proteasome-dependent ERAD (Werner *et al.*, 1996; Chillaron *et al.*, 2000). As shown in Figure 3B, levels of BiP expression did not change upon treatment of cells with kifunensine, swainsonine, or lactacystin.

To see if GFP-tagged $H2K^b$ heavy chains were resistant to proteasomal degradation, $\beta2m^{-/-}$ cells were pulse-chased in the presence and absence of lactacystin (Figure 3C). Using calnexin as a negative control for proteasomal degradation, both $H2K^b$ and $H2K^bGFP$ were significantly degraded after 4 h of chase (Figure 3C). Signal decay of $H2K^bGFP$ bands was twofold higher than that of calnexin bands, and lactacystin rescued both $H2K^b$ and $H2K^bGFP$ proteins from degradation. Thus, the lack of effect on $H2K^bGFP$ diffusion upon inhibition of ERAD was not due to disruption of the proteasomal degradation of GFP-tagged heavy chains.

Because lateral diffusion of transmembrane proteins is proportional to the logarithm of their radius (Hughes *et al.*, 1982), FRAP measurements will report similar diffusion coefficients for freely diffusing species whose radii differ by an order of magnitude. In addition, autofluorescence and discontinuities in ER tubules do not allow resolution of subtle differences in the mobile fraction of freely diffusing molecules. Therefore, clustering of unassembled MHC class I molecules cannot be ruled out.

To detect small clusters of unassembled/misfolded proteins, $H2K^b$ molecules were tagged with the cyan (CFP) and yellow (YFP) spectral variants of GFP, and these chimeras were transiently expressed in $\beta2m^{-/-}$ cells. Intramembrane

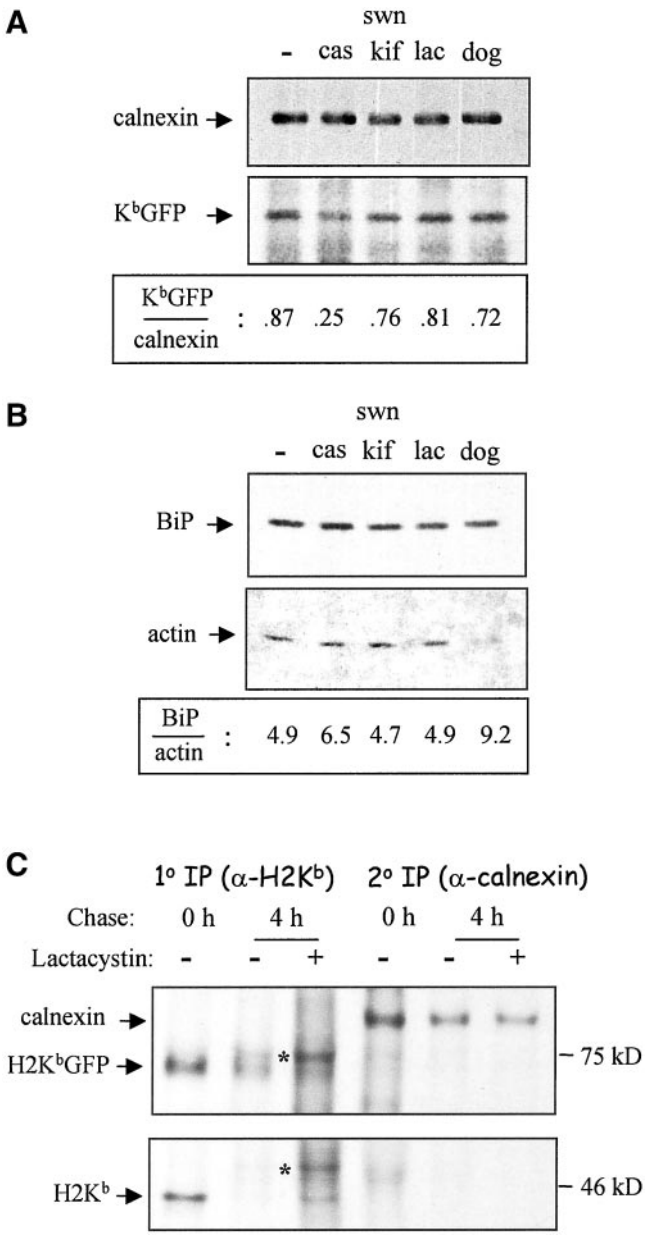

Figure 3. Association of H2K^{b}GFP with calnexin, and relative amounts of protein BiP expression. (A) $\beta 2m^{-/-}$K^{b}GFP cells were lysed in buffer containing 1% CHAPS, and lysates were incubated with an anticalnexin serum. Immunoprecipitates were resolved by electrophoresis on 7.5% SDS-PAGE, transferred to membranes, and probed with anticalnexin and anti-GFP. Densitometric analysis was performed to determine the ratio of H2K^{b}GFP to calnexin molecules. (B) $\beta 2m^{-/-}$K^{b}GFP cells were lysed in buffer containing 1% CHAPS. A fraction of each lysate was electrophoresed on 12% SDS-PAGE, transferred to membranes, and probed with anti-Grp78 (BiP) and antiactin. Densitometric analysis was performed to determine the ratio of BiP to actin molecules. (C) $\beta 2m^{-/-}$K^{b}GFP cells were labeled with [^{35}S]methionine for 20 min and chased for 4 h in the presence or absence of 25 μM lactacystin. To recover unassembled MHC class I molecules, lysates were incubated with β2m and high-affinity peptide SIY. H2K^{b}GFP and calnexin molecules were sequentially precipitated with mAb 20-8-4 (1° IP) and anticalnexin (2° IP). The asterisk points to glycosylated forms of H2K^b and H2K^{b}GFP molecules, which were largely unprocessed at 0 h of chase. Pharmacological treatments: cas, 1 mM castanospermine for 90 min; swn/kif, 1 mM swainsonine and 1 mM kifunensine for 90 min; lac, 20 μM lactacystin for 90 min; dog, 50 mM 2-deoxy-D-glucose and 0.02% sodium azide in glucose- and sodium pyruvate-free medium for 45 min.

distribution of H2K^{b}CFP and H2K^{b}YFP was imaged by FRET microscopy, a method that was recently used to show clustering of fully assembled MHC class I molecules for export from the ER (Pentcheva and Edidin, 2001). In FRET, the energy that is transferred nonradiatively from an H2K^{b}CFP molecule (donor) to an H2K^{b}YFP molecule (acceptor) results in apparent quenching of CFP fluorescence. FRET then is measured as the percent increase in donor fluorescence intensity after the acceptor is destroyed by photobleaching. Because energy transfer decays with the sixth power of the donor-to-acceptor distance, FRET is detected only when acceptor and donor are ~100 Å or less apart.

If H2K^{b}CFP and H2K^{b}YFP molecules are clustered, FRET is predicted to be independent of acceptor concentration and to increase with high ratios of acceptor-to-donor fluorophores (Kenworthy and Edidin, 1998; Pentcheva and Edidin, 2001). In contrast, if H2K^{b}CFP and H2K^{b}YFP molecules are randomly distributed, FRET is predicted to increase with increasing acceptor concentration and to be independent of acceptor-to-donor ratios (Kenworthy and Edidin, 1998; Pentcheva and Edidin, 2001). For a mixed population of clustered and randomly distributed molecules, FRET is expected to be dependent on both acceptor concentration and ratio of acceptor to donor fluorophores (Kenworthy and Edidin, 1998; Pentcheva and Edidin, 2001).

In separate transfections, three different ratios (2:1, 1:1, and 1:2) of plasmids encoding for H2K^{b}YFP and H2K^{b}CFP were introduced in $\beta 2m^{-/-}$ cells. To confirm that these ratios were maintained during expression of H2K^b molecules, the ratio of prebleach YFP fluorescence to postbleach CFP fluorescence was calculated, and it was found that the range of values for this ratio was characteristic of a particular transfection. In Figure 4, the percent of energy transfer between H2K^{b}YFP and H2K^{b}CFP molecules increased with increasing concentration of H2K^{b}YFP. However, FRET did not change with increasing ratios of acceptor to donor fluorophores. Thus, unassembled/misfolded H2K^b molecules did not appear to cluster in subnanometer membrane domains. Random distribution of unassembled MHC class I molecules persisted upon treatment of $\beta 2m^{-/-}$ cells with castanospermine, swainsonine/kifunensine, and lactacystin (Figure 4, B–D).

Segregation of MHC Class I Molecules into a Distinct ER Membrane Domain of ATP-depleted $\beta 2m^{-/-}$ Cells

Intracellular ATP has been proposed to regulate the binding capacity of ER-resident chaperones such as BiP and calnexin (Hendershot et al., 1996; Ihara *et al.*, 1999), the assembly of the ERAD machinery (McCracken and Brodsky, 1996; Wilson *et al.*, 2000), and perhaps, through these, the structure of

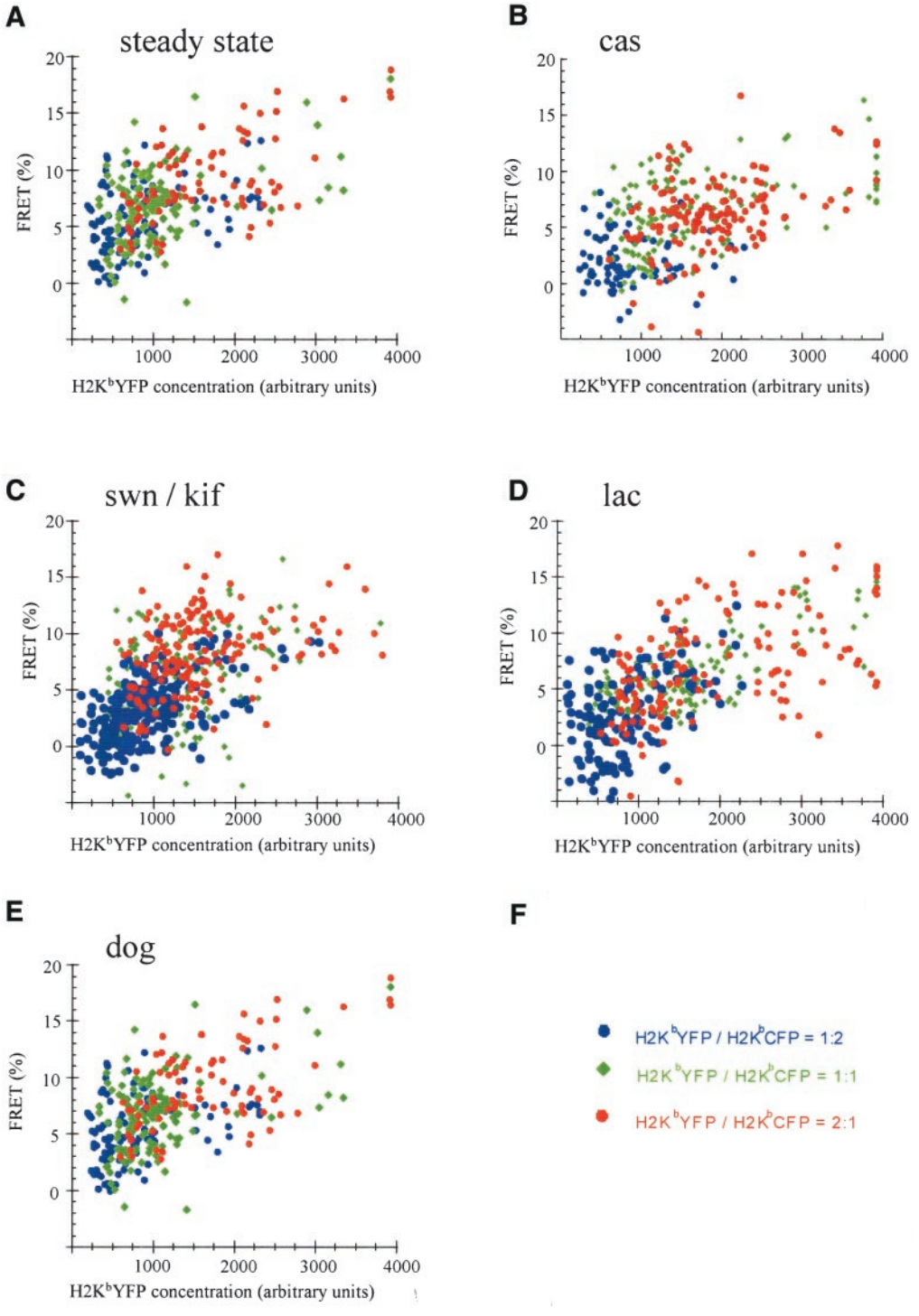

Figure 4. Random distribution of unassembled H2K^b molecules in the ER membrane of $\beta 2m^{-/-}$ cells. $\beta 2m^{-/-}$ cells were transfected with plasmid DNAs encoding for H2K^{b}YFP and H2K^{b}CFP at the ratios of 2:1 (red circles), 1:1 (green rhombs), and 1:2 (blue circles). After 36 h, cells were fixed and imaged by FRET microscopy (see MATERIALS AND METHODS). Each point represents the percent increase in H2K^{b}CFP fluorescence after the photobleaching of H2K^{b}YFP and the mean value of H2K^{b}YFP fluorescence (acceptor concentration), before photobleaching. These values were calculated for 5 × 5-pixel (340 × 340 nm) areas of the perinuclear ER. In all conditions, FRET depended on the concentration of H2K^{b}YFP and was independent of the ratio of acceptor to donor fluorophores. Results are representative of two or more experiments with similar outcomes. (A) Untreated; (B) 1 mM castanospermine for 90 min; (C) 1 mM swainsonine and 1 mM kifunensine for 90 min; (D) 20 μM lactacystin for 90 min; (E) 50 mM 2-deoxy-D-glucose and 0.02% sodium azide in glucose- and sodium pyruvate-free medium for 45 min.

an ER matrix (Hendershot *et al.*, 1995; Tatu and Helenius, 1997). Because separately, inhibition of MHC class I-calnexin association and suppression of ERAD did not have any effect on the dynamic mechanism of ER retention, their collective involvement was assessed by depriving $\beta 2m^{-/-}$ cells of metabolic energy.

On incubating cells in glucose-free medium containing 2-deoxy-D-glucose (dog) and sodium azide, there was a 20% decrease in the association of H2K^{b}GFP molecules with calnexin (Figure 3A). Furthermore, the amount of BiP protein doubled (Figure 3B), which was consistent with previous reports showing elevated BiP expression in response to glucose deprivation and defective protein folding (Pouyssegur *et al.*, 1977; Kozutsumi *et al.*, 1988). Measurements of lateral diffusion showed a twofold reduction in the mobile fraction of H2K^{b}GFP molecules (Table 1), which was suggestive of aggregation or irreversible association with immobile components of the ER. However, FRET microscopy failed to detect any clustering, and the immobile species maintained random distribution within the ER membrane of ATP-depleted cells (Figure 4E).

Because aggregation of unassembled molecules was inconsistent with lack of clustering, ER membrane morphology was examined for distortions, which may have caused the apparent low mobility of H2K^{b}GFP by isolating them in domains. Untreated and ATP-depleted $\beta 2m^{-/-}$ (untransfected) cells were labeled with the fluorescent dye DiOC6, which stains the ER and mitochondria of fixed cells (Terasaki *et al.*, 1986). DiOC6-labeled cells were imaged by deconvolution microscopy. ATP-depleted cells appeared smaller in size, and their ER was somewhat retracted from the periphery of the cell; however, no obvious defects such as vesiculation and fragmentation were observed (our unpublished results). Consistent with these observations, the diffusion of a small lipophilic probe was recently shown to remain unchanged upon ATP depletion, suggesting that ER membrane geometry does not account for low fluorescence recovery (Levin *et al.*, 2001).

To explore the possibility that unassembled/misfolded molecules were segregated into subregions of the ER where they remained randomly distributed, $\beta 2m^{-/-}$ K^{b}GFP cells were imaged by confocal microscopy. In ATP-depleted cells, H2K^{b}GFP molecules lost their reticular distribution (Figure 5, A and G) and appeared to accumulate in a juxtanuclear region of at least 5 μm in diameter (Figure 5, D and J). Some H2K^{b}GFP fluorescence was observed in tubular elements throughout the cytosol. In this dramatic redistribution, MHC class I molecules were accompanied by calnexin, which maintained nearly perfect colocalization with H2K^{b}GFP (Figure 5F). Within 30 min after the return of cells to glucose-containing medium, H2K^{b}GFP molecules assumed their original reticular distribution (our unpublished results). Therefore, the region of MHC class I/calnexin accumulation appeared to be an ER-associated membrane domain.

The location of this domain with respect to the Golgi apparatus was examined by staining for the medial- and trans-Golgi marker protein α-mannosidase II. In untreated cells, α-mannosidase II was predominately localized to juxtanuclear ribbon-like elements reminiscent of Golgi stacks (Figure 5H, arrow). On ATP-depletion, α-mannosidase II did not change its juxtanuclear position. However, the ribbon-like elements became discontinuous (Figure 5, K and L) and they appeared to be at the periphery of the region where H2K^{b}GFP molecules were heavily accumulated (see inset in Figure 5L).

To see if this region was a distinct ER membrane domain associated with the transitional ER (ER-exit sites) or the ERGIC, ATP-depleted $\beta 2m^{-/-}$K^{b}GFP cells were stained for p137 and p58. The p58-stained ERGIC elements lost their compact juxtanuclear localization (Figure 1H), and they appeared scattered throughout the cytosol (Figure 6B). These structures were clearly excluded from H2K^{b}GFP-containing regions (Figure 6C). In contrast, although some p137 puncta were seen, presumably at exit sites, most of the p137 molecules became concentrated in regions that contained H2K^{b}GFP (Figure 6F). The position and extent of these areas were similar to that observed for concentrations of calnexin and H2K^{b}GFP (Figure 5F) and are therefore distinct from classical ER exit sites. This juxtanuclear concentration of MHC class I and COPII molecules was dependent on microtubules. When cells were depleted of ATP in the presence of nocodazole, H2K^{b}GFP appeared in local patches throughout the cytoplasm but did not collapse to a single juxtanuclear region (Figure 6G). COPII puncta remained throughout the cytoplasm (Figure 6H), and only a fraction of H2K^{b}GFP molecules colocalized with perinuclear patches of COPII (yellow in Figure 6I). This effect was specific to ATP depletion, because treatment of cells with nocodazole alone had no effect (our unpublished results).

To see if our observations were due to the collapse of the ER around the microtubuke organizing center (MTOC), ATP-depleted $\beta 2m^{-/-}$ cells that expressed native H2L^d molecules were labeled with DiOC6 and stained for unassembled H2L^d (Figure 6, J and K). As shown in Figure 6L, the region where MHC class I molecules accumulated occupied only a fraction of the overall DiOC6-stained ER membrane. Furthermore, when H2L^d expressing $\beta 2m^{-/-}$ cells were stained for the glycoprotein glucosyltransferase, a soluble ER-resident protein, the peripheral ER was visibly intact (see reticular morphology in the inset of Figure 7A), despite heavy accumulation of H2L^d molecules in a juxtanuclear region (Figure 7B). As shown in Figure 7C, extended regions of the peripheral ER (in green) did not contain any H2L^d fluorescence (in yellow). Because upon prolonged inhibition of proteasome activity, free MHC class I heavy chains have been observed to accumulate in a novel ER quality control compartment that contains ER resident chaperones including calnexin (Kamhi-Nesher *et al.*, 2001), we asked if this compartment contained COPII similar to our observations in ATP-depleted cells. Indeed, upon treating $\beta 2m^{-/-}$K^{b}GFP cells with lactacystin for 4 h, H2K^{b}GFP molecules accumulated in a juxtanuclear compartment that contained COPII (Figure 7, D–F). Therefore, concentration of MHC class I molecules, ER-resident chaperones, and COPII in an ER-associated compartment was not due to a nonspecific collapse of the ER. As shown in Figure 7, G–L, this compartment was also present in β2m-expressing L-cells, where H2K^{b}GFP molecules are not targeted for proteasomal degradation. ATP depletion of L-cells caused significant accumulation of H2K^{b}GFP and calnexin molecules in a juxtanuclear ER subcompartment (Figure 7, J–L).

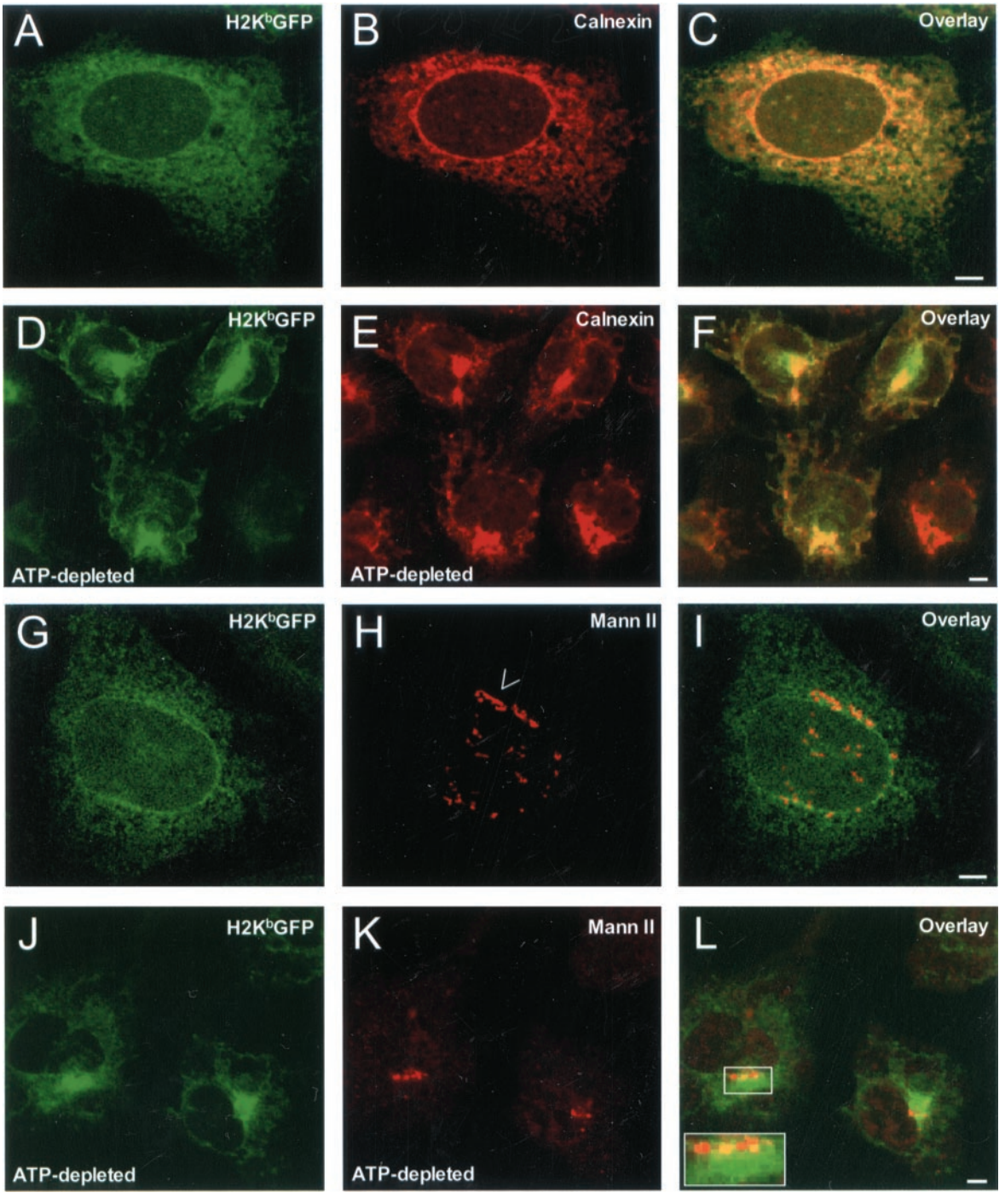

Figure 5. Intracellular distribution of H2K^{b}GFP, calnexin, and mannosidase II in untreated and ATP-depleted $\beta 2m^{-/-}$ cells. $\beta 2m^{-/-}$K^{b}GFP cells were fixed, permeabilized, and stained with anticalnexin and Cy5-conjugated anti-rabbit Ig. (A) H2K^{b}GFP; (B) calnexin; and (C) overlay of A and B. $\beta 2m^{-/-}$K^{b}GFP cells were incubated in glucose- and sodium pyruvate-free medium containing 50 mM 2-deoxy-D-glucose and 0.02% sodium azide (ATP-depletion medium) for 45 min. Subsequently, cells were fixed, permeabilized, and stained with anticalnexin and Cy5-conjugated anti-rabbit Ig. (D) H2K^{b}GFP; (E) calnexin; and (F) overlay of D and E. $\beta 2m^{-/-}$K^{b}GFP cells were fixed, permeabilized, and stained with anti–α-mannosidase II and Cy5-conjugated anti-rabbit Ig. (G) H2K^{b}GFP; (H) α-mannosidase II; and (I) overlay of G and H. $\beta 2m^{-/-}$K^{b}GFP cells were incubated in ATP-depletion medium for 45 min. Subsequently, cells were fixed, permeabilized, and stained with anti–α-mannosidase II and Cy5-conjugated anti-rabbit Ig. (J) H2K^{b}GFP; (K) α-mannosidase II; and (L) overlay of J and K. Arrow, an intact stack(s) of the Golgi complex stained for α-mannosidase II; inset, higher magnification of a broken Golgi ribbon adjacent to the region of H2K^{b}GFP accumulation. All images represent ~1-μm optical sections obtained by confocal microscopy. Scale bars, ~5 μm.

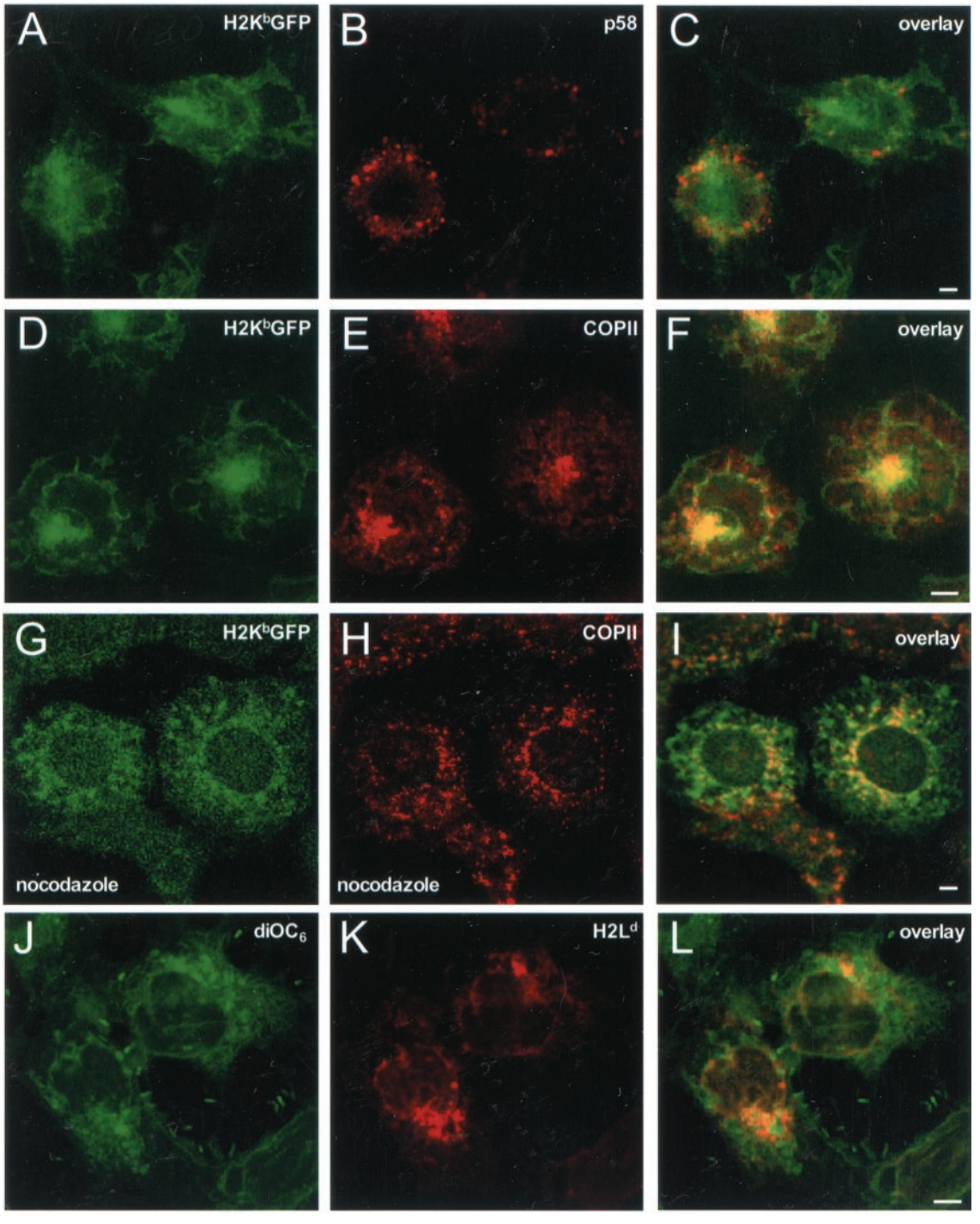

Figure 6. ER membrane localization of H2K^{b}GFP in ATP-depleted $\beta2m^{-/-}$ cells. $\beta2m^{-/-}$K^{b}GFP cells were incubated in ATP-depletion medium for 45 min. Subsequently, cells were fixed, permeabilized, and stained with anti-p58 and Cy5-conjugated anti-rabbit Ig. (A) H2K^{b}GFP; (B) p58; and (C) overlay of A and B. $\beta2m^{-/-}$K^{b}GFP cells were incubated in ATP-depletion medium for 45 min. Subsequently, cells were fixed, permeabilized, and stained with anti-p137 and Cy5-conjugated anti-rabbit Ig. (D) H2K^{b}GFP; (E) p137; and (F) overlay of D and E. $\beta2m^{-/-}$K^{b}GFP cells were treated with nocodazole for 1 h and then switched to ATP-depletion medium containing 33 μM nocodazole for 45 min. Subsequently, cells were fixed, permeabilized, and stained with anti-p137 and Cy5-conjugated anti-rabbit Ig. (G) H2K^{b}GFP; (H) p137; and (I) overlay of G and H. $\beta2m^{-/-}$ cells were transfected with *H2L^d*, and after 36 h of expression, they were incubated in ATP-depletion medium for 45 min. Subsequently, cells were fixed, permeabilized, and stained with mAb 64-3-7 (antiunfolded H2L^d) and Cy5-conjugated anti-mouse Ig. Samples were sequentially stained with DiOC6. (J) DiOC6; (K) H2L^d; and (L) overlay of J and K. All images represent ~1-μm optical sections obtained by confocal microscopy. Scale bars, ~5 μm.

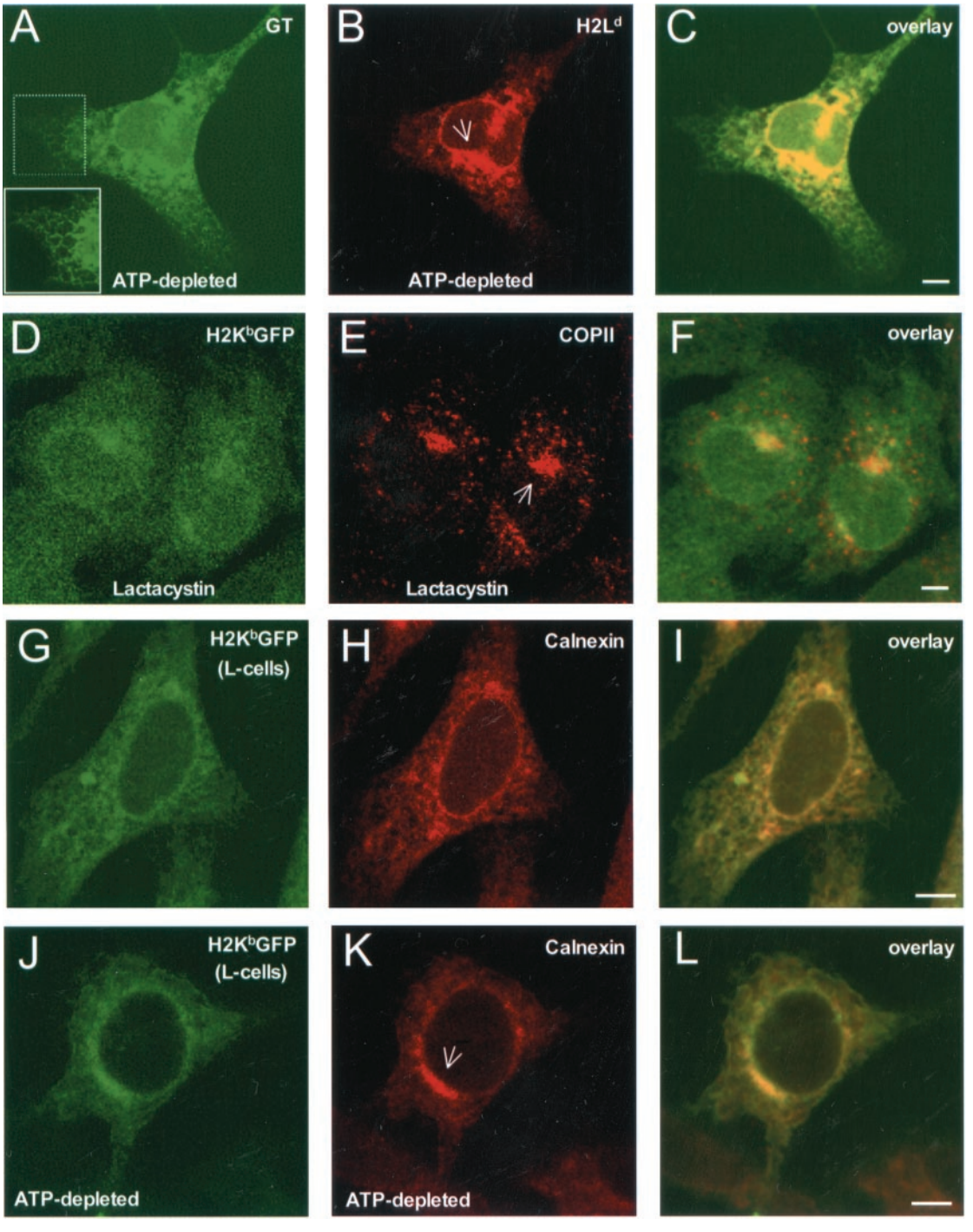

Figure 7. Redistribution of MHC class I molecules and chaperones in a distinct ER subdomain. $\beta 2m^{-/-}$ cells were transfected with *H2L*^{d}, and after 36 h of expression, they were incubated in ATP-depletion medium for 45 min. Subsequently, cells were fixed, permeabilized, and stained with a mixture of mAb 64-3-7 (antiunfolded H2L^d) and anti-UDPGlc:glycoprotein glucosyltransferase (GT), followed by Cy5-conjugated anti-mouse Ig and Alexa 488–conjugated anti-rabbit Ig. (A) glucosyltransferase; (B) H2L^d; and (C) overlay of A and B. $\beta 2m^{-/-}$K^{b}GFP cells were treated with lactacystin (25 μM) for 4 h. Subsequently, cells were fixed, permeabilized, and stained with anti-p137 and Cy5-conjugated anti-rabbit Ig. (D) H2K^{b}GFP; (E) p137; and (F) overlay of D and E. L-cells were transfected with *pH2K^{b}GFP*, and after 36 h of expression, they were fixed, permeabilized, and stained with anticalnexin and Cy5-conjugated anti-rabbit Ig. (G) H2K^{b}GFP; (H) calnexin; and (I) overlay of G and H. The same was repeated for L-cell transfectants, which were incubated in ATP-depletion medium for 2 h. (J) H2K^{b}GFP; (K) calnexin; and (L) overlay of J and K. Inset, higher magnification of a peripheral ER region with reticular morphology; arrows in B, E, and K, a novel ER-associated compartment (see text). The images shown represent ~1-μm optical sections obtained by confocal microscopy. Scale bars, ~5 μm.

DISCUSSION

Although much is known about assembly and ER-export of nascent proteins, there is a dearth of information about the mechanism(s) that mediate ER retention and degradation of unassembled/misfolded molecules. Moreover, it is unknown how the ER membrane is organized to retain and purge defective products of protein synthesis without disrupting normal biosynthesis and export.

Here, the intramembrane milieus of the ER were probed by visualizing the mobility and distribution of unassembled MHC class I molecules in β2m-deficient cells. Unfolded molecules did not exit the ER. The mechanism of restriction appeared to be highly dynamic, and it did not involve sequestration or clustering into distinct membrane domains. It was reasoned that the dynamic phenotype might be due to association with ER-resident chaperones and the molecular machinery of ERAD. However, upon inhibition of these processes, no visible change was observed. To assess if this phenotype was sustained by ER-resident factors that require a continuous input of metabolic energy, cells were deprived of ATP. Unassembled molecules became immobile and were found sequestered in an ER-associated membrane domain.

Previous studies have indicated that misfolded MHC class I proteins are predominately localized to the ERGIC (Hsu *et al.*, 1991; Baas *et al.*, 1992; Raposo *et al.*, 1995). In these reports, only Hsu *et al.* (1991) examined localization of MHC class I molecules in response to defective association with β2m. By using an interferon-γ–inducible carcinoma cell line, the authors concluded that unassembled $H2K^d$ molecules rapidly recycle between the ER and the Golgi apparatus. Although some unassembled MHC class I molecules are found at ER-exit sites and the ERGIC, our results show that most unfolded molecules do not accumulate at exit sites and do not leave the ER. This discrepancy may be due to differences in the cell lines and the MHC class I alleles used (Potter *et al.*, 1984; Klar and Hammerling, 1989). However, exclusion of unassembled MHC class I molecules from vesicular traffic agrees with recent evidence showing that in contrast to the degradation of soluble proteins, vesicular transport between the ER and the Golgi is not required for degradation of transmembrane proteins (Caldwell *et al.*, 2001; Vashist *et al.*, 2001).

Consistent with reports on the intramembrane mobility of ts045 VSVG, a misfolded protein that also fails to exit the ER (Storrie *et al.*, 1994; Nehls *et al.*, 2000), MHC class I molecules were highly mobile in the ER membrane of $\beta 2m^{-/-}$ cells. FRET microscopy ruled out the possibility that unassembled molecules clustered into rapidly diffusing aggregates of ≤100 Å in diameter. However, dimeric association of unassembled heavy chains cannot be ruled out (Capps *et al.*, 1993; Vassilakos *et al.*, 1996). Detection of clusters by FRET depends on the ratio of acceptor to donor fluorophores; therefore, dimeric associations, whose 1:1 ratio is always the same, will give the same FRET curves as a random distribution of monomers. Dimerization may also account for the lack of aggregation or clustering, upon treatment of cells with castanospermine.

It is also possible that calnexin-free MHC class I heavy chains were degraded or simply became associated with other ER-resident chaperones. Several studies have shown accelerated degradation of misfolded molecules in response to treatment with glucosidase inhibitors (Moore and Spiro, 1993; Hebert *et al.*, 1996; Wilson *et al.*, 2000). If MHC class I heavy chains were degraded, free cytosolic GFP should have increased the apparent D and R of $H2K^bGFP$. Therefore, it is more likely that after dissociation from calnexin, MHC class I molecules became associated with other ER-resident chaperones, which maintained a dynamic mechanism of ER-retention. In support of this interpretation, expression of MHC class I has been shown to proceed in the absence of glucose trimming and calnexin (Balow *et al.*, 1995; Scott and Dawson, 1995). Furthermore, elevated BiP expression was indicative of an induced unfolded protein response (UPR), which is known to upregulate the expression of several chaperones (Pouyssegur *et al.*, 1977; Kozutsumi *et al.*, 1988; Ng *et al.*, 2000). These proteins may compensate for loss of MHC class I association with calnexin.

On inhibition of ERAD, human MHC class I molecules have been observed to associate with ER-resident chaperones such as BiP, protein disulfide isomerase, and ERp57 (Wilson *et al.*, 2000). After treating $\beta 2m^{-/-}K^bGFP$ cells with inhibitors for ER mannosidases and the proteasome, lack of immobilization or clustering suggests that association with other chaperones prevented the aggregation of unfolded MHC class I molecules. Because recent evidence shows that Hsp70 facilitates the degradation of the cystic fibrosis transmembrane conductance regulator (CFTR; Zhang *et al.*, 2001), the role of cytosolic heat shock proteins cannot be excluded from such scenario. Overall, molecular chaperones appear to be intimately involved in the retrotranslocation and degradation of misfolded proteins (Nishikawa *et al.*, 2001); therefore, abolishing mannose trimming and proteasome activity may not alone be enough to cause aggregation and/or clustering of unassembled MHC class I molecules.

Our results suggest that high intramembrane mobility appears to be the preferred state for transmembrane proteins that are not properly folded. When cells are depleted of metabolic energy, unassembled molecules appear to segregate into an ER subdomain that contains calnexin and COPII, suggesting that this domain is associated with the rough and transitional ER.

The size and irregular shape of our calnexin/MHC class I-containing ER domain (Figures 5 and 6) are markedly different from CFTR-containing aggresomes (Johnston *et al.*, 1998), mutant huntingtin-containing degrasomes (Waelter *et al.*, 2001), and the β-COP–containing fibrillar aggregates of anoxic pancreatic acinar cells (Hendricks *et al.*, 1993). Rather, this membrane domain closely resembles a "quality control" compartment, which was recently found to contain calnexin and calreticulin, and the Sec61 translocon, as well as the precursor of the human asialoglycoprotein receptor H2a and free MHC class I heavy chains (Kamhi-Nesher *et al.*, 2001). Similar to the studies of Kamhi-Nesher *et al.* (2001), this compartment became visible only upon prolonged (4–5 h) inhibition of the proteasome, and here, it was shown to contain COPII (Figure 7, D–F).

Because, upon ATP-depletion, this compartment contained both calnexin and COPII, it appears to be an ER subdomain different from the COPII-containing ER exit sites, which at steady state do not include any calnexin molecules (Cannon and Helenius, 1999). Immuno-EM studies by Schekman and coworkers have revealed that ER exit sites are marked by a membrane bound fraction (~20%) and by a large cytoplasmic pool of COPII that appears to be

adjacent to membranes of the transitional zone, as if tethered to a cytoskeletal framework (Orci *et al.*, 1991). These cytosolic pools of COPII may be free to relocate on new membrane domains during ATP-depletion or treatment with lactacystin as shown in Figures 6, D–F, and 7, D–F, respectively. Segregation of unfolded MHC class I molecules into a distinct membrane domain may be a temporary adaptation to conditions of cell stress.

To conclude, in contrast to a model of molecular aggregation and sequestration (Hurtley and Helenius, 1989), unassembled and misfolded MHC class I proteins appear to maintain a state of high intramembrane mobility. The results of this work imply that several ATP-dependent mechanisms are in effect to maintain high mobility and random distribution of unfolded species. Perhaps, this is the most efficient method to degrade defective products of protein synthesis without interfering with normal biosynthesis. Recent studies indicate that restricted diffusion and clustering are respectively reserved for the assembly and ER-export of nascent MHC class I molecules (Marguet *et al.*, 1999; Spiliotis *et al.*, 2000; Pentcheva and Edidin, 2001). Therefore, ER membrane domains appear to mediate specialized events of protein biosynthesis such as oligomerization and export.

ACKNOWLEDGMENTS

The authors thank Drs. Ann Hubbard, Jaakko Saraste, Marilyn Farquhar, Ted Hansen, Armando Parodi, and Mark Terasaki for their kind donations of reagents; Dr. Stephen Gould for the SV40 T-Ag reagent and expert advice on cell transformation; Michael McCaffery and Gerry Sexton (The Johns Hopkins Integrated Imaging Center) for cell imaging by electron microscopy; Ms. Taiyin Wei and Dr. Qing Tang for various technical support; Drs. Martha Zúñiga (UCSC) and Carolyn Machamer (JHMI) for helpful comments and suggestions. This work was supported by National Institutes of Health grant AI14584 to M.E.

REFERENCES

Baas, E.J., van Santen, H.M., Kleijmeer, M.J., Geuze, H.J., Peters, P.J., and Ploegh, H.L. (1992). Peptide-induced stabilization and intracellular localization of empty HLA class I complexes. J. Exp. Med. *176*, 147–156.

Balow, J.P., Weissman, J.D., and Kearse, K.P. (1995). Unique expression of major histocompatibility complex class I proteins in the absence of glucose trimming and calnexin association. J. Biol. Chem. *270*, 29025–29029.

Baumann, O., and Walz, B. (2001). Endoplasmic reticulum of animal cells and its organization into structural and functional domains. Int. Rev. Cytol. *205*, 149–214.

Cabral, C.M., Choudhury, P., Liu, Y., and Sifers, R.N. (2000). Processing by endoplasmic reticulum mannosidases partitions a secretion- impaired glycoprotein into distinct disposal pathways. J. Biol. Chem. *275*, 25015–25022.

Caldwell, S.R., Hill, K.J., and Cooper, A.A. (2001). Degradation of ER quality control substrates requires transport between the ER and Golgi. J. Biol. Chem. *276*, 23296–23303.

Cannon, K.S., and Helenius, A. (1999). Trimming and readdition of glucose to N-linked oligosaccharides determines calnexin association of a substrate glycoprotein in living cells. J. Biol. Chem. *274*, 7537–7544.

Capps, G.G., Robinson, B.E., Lewis, K.D., and Zúñiga, M.C. (1993). In vivo dimeric association of class I MHC heavy chains. Possible relationship to class I MHC heavy chain-beta 2-microglobulin dissociation. J. Immunol. *151*, 159–169.

Chillaron, J., Adan, C., and Haas, I.G. (2000). Mannosidase action, independent of glucose trimming, is essential for proteasome-mediated degradation of unassembled glycosylated Ig light chains. Biol. Chem. *381*, 1155–1164.

Cresswell, P., Bangia, N., Dick, T., and Diedrich, G. (1999). The nature of the MHC class I peptide loading complex. Immunol. Rev. *172*, 21–28.

Ellgaard, L., Molinari, M., and Helenius, A. (1999). Setting the standards: quality control in the secretory pathway. Science *286*, 1882–1888.

Gonzalez, D.S., Karaveg, K., Vandersall-Nairn, A.S., Lal, A., and Moremen, K.W. (1999). Identification, expression, and characterization of a cDNA encoding human endoplasmic reticulum mannosidase I, the enzyme that catalyzes the first mannose trimming step in mammalian Asn-linked oligosaccharide biosynthesis. J. Biol. Chem. *274*, 21375–21386.

Hammond, A.T., and Glick, B.S. (2000). Dynamics of transitional endoplasmic reticulum sites in vertebrate cells. Mol. Biol. Cell *11*, 3013–3030.

Hebert, D.N., Foellmer, B., and Helenius, A. (1996). Calnexin and calreticulin promote folding, delay oligomerization and suppress degradation of influenza hemagglutinin in microsomes. EMBO J. *15*, 2961–2968.

Hendershot, L., Wei, J., Gaut, J., Melnick, J., Aviel, S., and Argon, Y. (1996). Inhibition of immunoglobulin folding and secretion by dominant negative BiP ATPase mutants. Proc. Natl. Acad. Sci. USA *93*, 5269–5274.

Hendershot, L.M., Wei, J.Y., Gaut, J.R., Lawson, B., Freiden, P.J., and Murti, K.G. (1995). In vivo expression of mammalian BiP ATPase mutants causes disruption of the endoplasmic reticulum. Mol. Biol. Cell *6*, 283–296.

Hendricks, L.C., McCaffery, M., Palade, G.E., and Farquhar, M.G. (1993). Disruption of endoplasmic reticulum to Golgi transport leads to the accumulation of large aggregates containing beta-COP in pancreatic acinar cells. Mol. Biol. Cell *4*, 413–424.

Hirsch, C., and Ploegh, H.L. (2000). Intracellular targeting of the proteasome. Trends Cell Biol. *10*, 268–272.

Hsu, V.W., Yuan, L.C., Nuchtern, J.G., Lippincott-Schwartz, J., Hammerling, G.J., and Klausner, R.D. (1991). A recycling pathway between the endoplasmic reticulum and the Golgi apparatus for retention of unassembled MHC class I molecules. Nature *352*, 441–444.

Hughes, B.D., Pailthorpe, B.A., White, L.R., and Sawyer, W.H. (1982). Extraction of membrane microviscosity from translational and rotational diffusion coefficients. Biophys. J. *37*, 673–676.

Hughes, E.A., Hammond, C., and Cresswell, P. (1997). Misfolded major histocompatibility complex class I heavy chains are translocated into the cytoplasm and degraded by the proteasome. Proc. Natl. Acad. Sci. USA *94*, 1896–1901.

Hurtley, S.M., and Helenius, A. (1989). Protein oligomerization in the endoplasmic reticulum. Annu. Rev. Cell Biol. *5*, 277–307.

Ihara, Y., Cohen-Doyle, M.F., Saito, Y., and Williams, D.B. (1999). Calnexin discriminates between protein conformational states and functions as a molecular chaperone in vitro. Mol. Cell *4*, 331–341.

Johnston, J.A., Ward, C.L., and Kopito, R.R. (1998). Aggresomes: a cellular response to misfolded proteins. J. Cell Biol. *143*, 1883–1898.

Kamhi-Nesher, S., Shenman, M., Tolchinsky, S., Vigodman Fromm, S., Ehrlich, R., and Lederkremer, G.Z. (2001). A novel quality control compartment derived from the endoplasmic reticulum. Mol. Biol. Cell *10*, 1711–1723.

Kenworthy, A.K., and Edidin, M. (1998). Distribution of a glycosylphosphatidylinositol-anchored protein at the apical surface of MDCK cells examined at a resolution of < 100 A using imaging fluorescence resonance energy transfer. J. Cell Biol. *142*, 69–84.

Klar, D., and Hammerling, G.J. (1989). Induction of assembly of MHC class I heavy chains with beta 2microglobulin by interferon-gamma. EMBO J. *8*, 475–481.

Koller, B.H., Marrack, P., Kappler, J.W., and Smithies, O. (1990). Normal development of mice deficient in beta 2M, MHC class I proteins and CD8+ T cells. Science *248*, 1227–1230.

Kozutsumi, Y., Segal, M., Normington, K., Gething, M.J., and Sambrook, J. (1988). The presence of malfolded proteins in the endoplasmic reticulum signals the induction of glucose-regulated proteins. Nature *332*, 462–464.

Lee, Y.K., Brewer, J.W., Hellman, R., and Hendershot, L.M. (1999). BiP and immunoglobulin light chain cooperate to control the folding of heavy chain and ensure the fidelity of immunoglobulin assembly. Mol. Biol. Cell *10*, 2209–2219.

Levin, M.H., Haggie, P.M., Vetrivel, L., and Verkman, A.S. (2001). Diffusion in the endoplasmic reticulum of an aquaporin-2 mutant causing human nephrogenic diabetes insipidus. J. Biol. Chem. *276*, 21331–21336.

Lie, W.R., Myers, N.B., Connolly, J.M., Gorka, J., Lee, D.R., and Hansen, T.H. (1991). The specific binding of peptide ligand to Ld class I major histocompatibility complex molecules determines their antigenic structure. J. Exp. Med. *173*, 449–459.

Liu, Y., Choudhury, P., Cabral, C.M., and Sifers, R.N. (1999). Oligosaccharide modification in the early secretory pathway directs the selection of a misfolded glycoprotein for degradation by the proteasome. J. Biol. Chem. *274*, 5861–5867.

Marguet, D., Spiliotis, E.T., Pentcheva, T., Lebowitz, M., Schneck, J., and Edidin, M. (1999). Lateral diffusion of GFP-tagged H2Ld molecules and of GFP-TAP1 reports on the assembly and retention of these molecules in the endoplasmic reticulum. Immunity *11*, 231–240.

McCracken, A.A., and Brodsky, J.L. (1996). Assembly of ER-associated protein degradation in vitro: dependence on cytosol, calnexin, and ATP. J. Cell Biol. *132*, 291–298.

Moore, S.E., and Spiro, R.G. (1993). Inhibition of glucose trimming by castanospermine results in rapid degradation of unassembled major histocompatibility complex class I molecules. J. Biol. Chem. *268*, 3809–3812.

Nehls, S., Snapp, E.L., Cole, N.B., Zaal, K.J., Kenworthy, A.K., Roberts, T.H., Ellenberg, J., Presley, J.F., Siggia, E., and Lippincott-Schwartz, J. (2000). Dynamics and retention of misfolded proteins in native ER membranes. Nat. Cell Biol. *2*, 288–295.

Ng, D.T., Spear, E.D., and Walter, P. (2000). The unfolded protein response regulates multiple aspects of secretory and membrane protein biogenesis and endoplasmic reticulum quality control. J. Cell Biol. *150*, 77–88.

Nishikawa, S., Fewell, S.W., Kato, Y., Brodsky, J.L., and Endo, T. (2001). Molecular chaperones in the yeast endoplasmic reticulum maintain the solubility of proteins for retrotranslocation and degradation. J. Cell Biol. *153*, 1061–1070.

Nossner, E., and Parham, P. (1995). Species-specific differences in chaperone interaction of human and mouse major histocompatibility complex class I molecules. J. Exp. Med. *181*, 327–337.

Orci, L., Ravazzola, M., Meda, P., Holcomb, C., Moore, H.P., Hicke, L., and Schekman, R. (1991). Mammalian Sec23p homologue is restricted to the endoplasmic reticulum transitional cytoplasm. Proc. Natl. Acad. Sci. USA *88*, 8611–8615.

Pahl, H.L., and Baeuerle, P.A. (1995). A novel signal transduction pathway from the endoplasmic reticulum to the nucleus is mediated by transcription factor NF-kappa B. EMBO J. *14*, 2580–2588.

Pentcheva, T., and Edidin, M. (2001). Clustering of peptide-loaded MHC class I molecules for ER export imaged by fluorescence resonance energy transfer (FRET). J. Immunol. *166*, 6625–6632.

Plutner, H., Davidson, H.W., Saraste, J., and Balch, W.E. (1992). Morphological analysis of protein transport from the ER to Golgi membranes in digitonin-permeabilized cells: role of the P58 containing compartment. J. Cell Biol. *119*, 1097–1116.

Potter, T.A., Boyer, C., Verhulst, A.M., Golstein, P., and Rajan, T.V. (1984). Expression of H-2Db on the cell surface in the absence of detectable beta 2 microglobulin. J. Exp. Med. *160*, 317–322.

Pouyssegur, J., Shiu, R.P., and Pastan, I. (1977). Induction of two transformation-sensitive membrane polypeptides in normal fibroblasts by a block in glycoprotein synthesis or glucose deprivation. Cell *11*, 941–947.

Pryme, I.F. (1986). Compartmentation of the rough endoplasmic reticulum. Mol Cell Biochem. *71*, 3–18.

Raposo, G., van Santen, H.M., Leijendekker, R., Geuze, H.J., and Ploegh, H.L. (1995). Misfolded major histocompatibility complex class I molecules accumulate in an expanded ER-Golgi intermediate compartment. J. Cell Biol. *131*, 1403–1419.

Rivera, V.M., Wang, X., Wardwell, S., Courage, N.L., Volchuk, A., Keenan, T., Holt, D.A., Gilman, M., Orci, L., Cerasoli, F., Jr., Rothman, J.E., and Clackson, T. (2000). Regulation of protein secretion through controlled aggregation in the endoplasmic reticulum. Science *287*, 826–830.

Saraste, J., and Svensson, K. (1991). Distribution of the intermediate elements operating in ER to Golgi transport. J. Cell Sci. *100*, 415–430.

Scott, J.E., and Dawson, J.R. (1995). MHC class I expression and transport in a calnexin-deficient cell line. J. Immunol. *155*, 143–148.

Sege, K., Rask, L., and Peterson, P.A. (1981). Role of beta2-microglobulin in the intracellular processing of HLA antigens. Biochemistry *20*, 4523–4530.

Shiroishi, T., Evans, G.A., Appella, E., and Ozato, K. (1985). In vitro mutagenesis of a mouse MHC class I gene for the examination of structure-function relationships. J. Immunol. *134*, 623–629.

Shugrue, C.A., Kolen, E.R., Peters, H., Czernik, A., Kaiser, C., Matovcik, L., Hubbard, A.L., and Gorelick, F. (1999). Identification of the putative mammalian orthologue of Sec31P, a component of the COPII coat. J. Cell Sci. *112*, 4547–4556.

Spiliotis, E.T., Manley, H., Osorio, M., Zúñiga, M.C., and Edidin, M. (2000). Selective export of MHC class I molecules from the ER after their dissociation from TAP. Immunity *13*, 841–851.

Storrie, B., Pepperkok, R., Stelzer, E.H., and Kreis, T.E. (1994). The intracellular mobility of a viral membrane glycoprotein measured by confocal microscope fluorescence recovery after photobleaching. J. Cell Sci. *107*, 1309–1319.

Tatu, U., and Helenius, A. (1997). Interactions between newly synthesized glycoproteins, calnexin and a network of resident chaperones in the endoplasmic reticulum. J. Cell Biol. *136*, 555–565.

Terasaki, M., Chen, L.B., and Fujiwara, K. (1986). Microtubules and the endoplasmic reticulum are highly interdependent structures. J. Cell Biol. *103*, 1557–1568.

Tokunaga, F., Brostrom, C., Koide, T., and Arvan, P. (2000). Endoplasmic reticulum (ER)-associated degradation of misfolded N-linked glycoproteins is suppressed upon inhibition of ER mannosidase I. J. Biol. Chem. *275*, 40757–40764.

Vashist, S., Kim, W., Belden, W.J., Spear, E.D., Barlowe, C., and Ng, D.T. (2001). Distinct retrieval and retention mechanisms are re-

quired for the quality control of endoplasmic reticulum protein folding. J. Cell Biol. *155*, 355–368.

Vassilakos, A., Cohen-Doyle, M.F., Peterson, P.A., Jackson, M.R., and Williams, D.B. (1996). The molecular chaperone calnexin facilitates folding and assembly of class I histocompatibility molecules. EMBO J. *15*, 1495–1506.

Velasco, A., Hendricks, L., Moremen, K.W., Tulsiani, D.R., Touster, O., and Farquhar, M.G. (1993). Cell type-dependent variations in the subcellular distribution of alpha- mannosidase I and II. J. Cell Biol. *122*, 39–51.

Vertel, B.M., Walters, L.M., and Mills, D. (1992). Subcompartments of the endoplasmic reticulum. Semin. Cell Biol. *3*, 325–341.

Waelter, S., Boeddrich, A., Lurz, R., Scherzinger, E., Lueder, G., Lehrach, H., and Wanker, E.E. (2001). Accumulation of mutant huntingtin fragments in aggresome-like inclusion bodies as a result of insufficient protein degradation. Mol. Biol. Cell *12*, 1393–1407.

Wang, J., and White, A.L. (2000). Role of calnexin, calreticulin, and endoplasmic reticulum mannosidase I in apolipoprotein(a) intracellular targeting. Biochemistry *39*, 8993–9000.

Werner, E.D., Brodsky, J.L., and McCracken, A.A. (1996). Proteasome-dependent endoplasmic reticulum-associated protein degradation: an unconventional route to a familiar fate. Proc. Natl. Acad. Sci. USA *93*, 13797–13801.

Williams, D.B., Barber, B.H., Flavell, R.A., and Allen, H. (1989). Role of β2m-microglobulin in the intracellular transport and surface expression of murine class I histocompatibility complex molecules. J. Immunol. *142*, 2796–2806.

Wilson, C.M., Farmery, M.R., and Bulleid, N.J. (2000). Pivotal role of calnexin and mannose trimming in regulating the endoplasmic reticulum-associated degradation of major histocompatibility complex class I heavy chain. J. Biol. Chem. *275*, 21224–21232.

Yechiel, E., and Edidin, M. (1987). Micrometer-scale domains in fibroblast plasma membranes. J. Cell Biol. *105*, 755–760.

Zhang, Y., Nijbroek, G., Sullivan, M.L., McCracken, A.A., Watkins, S.C., Michaelis, S., and Brodsky, J.L. (2001). Hsp70 molecular chaperone facilitates endoplasmic reticulum-associated protein degradation of cystic fibrosis transmembrane conductance regulator in yeast. Mol. Biol. Cell. *12*, 1303–1314.

Zijlstra, M., Bix, M., Simister, N.E., Loring, J.M., Raulet, D.H., and Jaenisch, R. (1990). Beta 2-microglobulin deficient mice lack CD4–8+ cytolytic T cells. Nature *344*, 742–746.

Zuber, C., Fan, J., Guhl, B., Parodi, A., Fessler, J.H., Parker, C., and Roth, J. (2001). Immunolocalization of UDP-glucose:glycoprotein glucosyltransferase indicates involvement of pre-Golgi intermediates in protein quality control. Proc. Natl. Acad. Sci. USA *98*, 10710–10715.